Synthesis and structural characterization of mesitylphosphinidene-capped ruthenium and osmium clusters

Taeko Kakizawa, Hisako Hashimoto *, Hiromi Tobita *

Department of Chemistry, Graduate School of Science, Tohoku University, Aoba-ku, Sendai, Miyagi 980-8578, Japan

Abstract

Thermal reaction of $[Ru_3(CO)_{12}]$ with PH_2Mes (Mes = mesityl) in refluxing toluene afforded mesitylphosphinidene-capped ruthenium carbonyl clusters, $[Ru_3(CO)_9(\mu-H)_2(\mu_3-PMes)]$ (**1**), $[Ru_3(CO)_8(PH_2Mes)(\mu-H)_2(\mu_3-PMes)]$ (**2**), $[Ru_3(CO)_9(\mu_3-PMes)_2]$ (**3**), $[Ru_4(CO)_{10}(\mu-CO)(\mu_4-PMes)_2]$ (**4**), and $[Ru_5(CO)_{10}H_2(\mu_4-PMes)(\mu_3-PMes)_2]$ (**5**). All products were fully characterized and structurally confirmed by X-ray crystal structure analysis. Complexes **2**–**4** were also obtained in high yields by stepwise reaction starting from **1**. Fluxional behavior of carbonyl groups was observed in case of **4**. Complex **5** reveals a new type of skeletal structure, bicapped-octahedron having μ_3- and μ_4-phosphinidene ligands at the capping positions. Similar reaction of $[Os_3(CO)_{12}]$ with PH_2Mes yielded a phosphido-bridged osmium cluster $[Os_3(CO)_{10}(\mu-H)(\mu-PHMes)]$ (**6**) and a phosphinidene-capped cluster $[Os_3(CO)_9(\mu-H)_2(\mu_3-PMes)]$ (**7**).
© 2005 Elsevier B.V. All rights reserved.

Keywords: Cluster; Mesitylphosphine; Phosphinidene ligand; X-ray structure study

1. Introduction

Phosphinidene is a good tool for assembling metal fragments to build up metal clusters, since it can work as a four-electron donor and is capable of bridging two or more metal atoms. This interesting ligand can be conveniently generated from primary phosphines through their coordination to metal and the following dehydrogenation [1]. Huttner et al. and some other groups [2] have proved that thermolysis of $[M_3(CO)_{12}]$ (M = Fe, Ru, and Os) in the presence of a primary phosphine gives various Group 8 metal clusters bridged by phosphinidene ligands. Particularly, Smit et al. [3] successfully synthesized a wide range of ruthenium clusters with higher nuclearity containing phenylphosphinidene ligands, i.e., $[Ru_4(CO)_{10}(\mu-CO)(\mu_4-PPh)_2]$, $[Ru_4(CO)_8(\mu-PPhH)_2(\mu_4-PPh)_2]$, $[Ru_5(CO)_{15}(\mu_4-PPh)]$, $[Ru_6(CO)_{12}(\mu_4-PPh)_3(\mu_3-PPh)_2]$, and $[Ru_6(CO)_{12}(\mu_4-PPh)_2(\mu_3-PPh)_2]$, etc.

However, since the variety of primary phosphines used for bridging-ligand precursors is still limited, the research in this area is yet at the early stage of development.

In the chemistry of phosphinidene-capped metal clusters, the substituent on phosphorus can be a critical factor for growth of the cluster framework. In this work, we performed cluster syntheses of ruthenium and osmium with use of mesitylphosphine PH_2Mes (Mes = 2,4,6-trimethylphenyl = mesityl) as a precursor of the bridging unit [4]. Although a few examples of mesitylphosphinidene-capped carbonyl clusters of iron are known (i.e., $[Fe_3(CO)_9(\mu-CO)(\mu_3-PMes)]$ [5] and $[Fe_3(CO)_9(\mu_3-PMes)_2]$ [6]), no examples of mesitylphosphinidene-ruthenium or -osmium clusters have been reported. The influence of the bulky mesityl group upon the skeletal structure of the clusters is of interest. In fact, our trial gave a ruthenium compound having a new type of core structure besides species with known frameworks. This paper describes the full characterization of seven mesitylphosphinidene-capped ruthenium and osmium clusters. Stepwise and high-yield transformation reactions of obtained complexes are also described.

2. Results and discussion

2.1. Synthesis and structures of ruthenium clusters 1–5

Heating a toluene solution containing PH_2Mes and $[Ru_3(CO)_{12}]$ in a 1:1 molar ratio produced a mixture of tri-ruthenium complexes $[Ru_3(CO)_9(\mu\text{-}H)_2(\mu_3\text{-}PMes)]$ (**1**), $[Ru_3(CO)_8(PH_2Mes)(\mu\text{-}H)_2(\mu_3\text{-}PMes)]$ (**2**), and $[Ru_3(CO)_9(\mu_3\text{-}PMes)_2]$ (**3**), a tetraruthenium complex $[Ru_4(CO)_{10}(\mu\text{-}CO)(\mu_4\text{-}PMes)_2]$ (**4**), and a pentaruthenium cluster $[Ru_5(CO)_{10}H_2(\mu_4\text{-}PMes)(\mu_3\text{-}PMes)_2]$ (**5**) (Scheme 1). The formation ratio of these products slightly depends on the reaction conditions. When the reaction was carried out in refluxing toluene for 30 min, complexes **1**, **2**, **3**, **4**, and **5** were obtained in 27%, 8%, 15%, 2%, and 17% yields, respectively. The formation of clusters **4** and **5** is favored under more forced conditions. Thus, overnight refluxing of the reaction mixture gave complexes **1**, **3**, **4**, and **5** in 26%, 14%, 10%, and 31% yields, respectively. Complex **2** was not obtained under this condition. The use of twofold molar amount of PH_2Mes under the same condition

produced complexes **1**, **3**, **4**, and **5** in 12%, 13%, 7%, and 33% yields, respectively, with unidentified oily products. When a reaction was carried out at lower temperature, i.e., in refluxing hexane, complex **2** was obtained in the yield higher than any other products [**1** (11%), **2** (29%), **3** (8%), **4** (4%), and **5** (5%)].

In a field of the synthesis of metal clusters, it is still difficult to obtain a desired cluster selectively in high yield and the formation mechanism of the products is not clear in many cases. Therefore, to find the ways to build up a target cluster efficiently is still one of the important research topics in this field. Although complexes **2**–**4** were obtained in only low yields from the above reactions, we found that they could be prepared selectively in high yields from complex **1** by the stepwise reactions shown in Scheme 2. Thus, complex **2** was obtained by the reaction of **1** with PH_2Mes in refluxing hexane in 78% yield. Overnight refluxing of a toluene solution of **2** under CO atmosphere gave **3** in 56% yield. Complex **3** reacted with $[Ru_3(CO)_{12}]$ in refluxing toluene to form tetraruthenium cluster **4** in 78% yield.
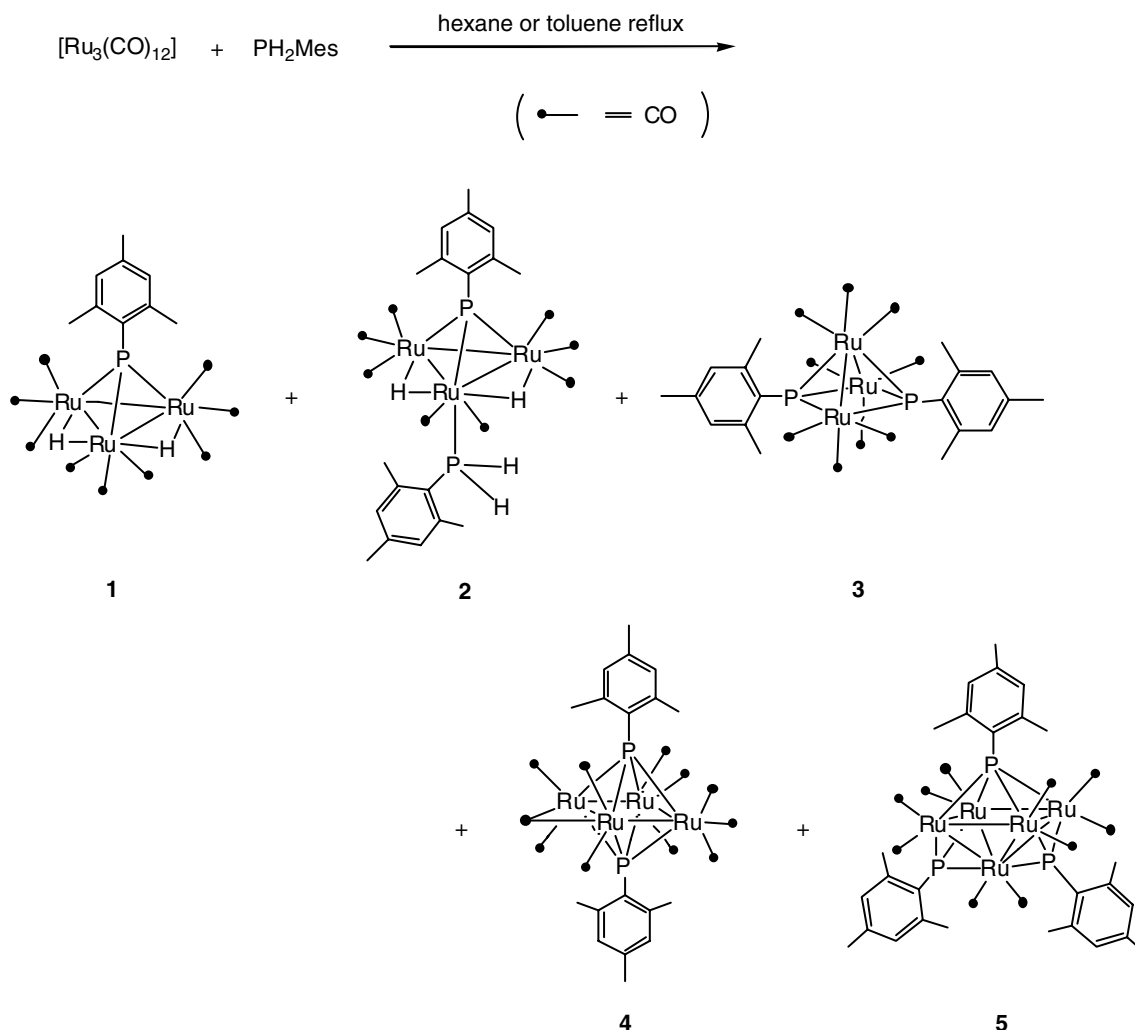
Scheme 1. Reaction of $[Ru_3(CO)_{12}]$ with PH_2Mes (hydride ligands on cluster **5** are not located).
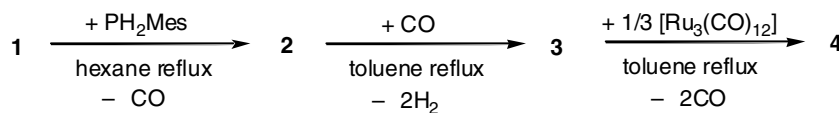
Scheme 2. Stepwise reactions starting from complex **1**.

Although we have not yet established the high-yield synthesis of the new cluster **5**, these results provide good evidences of the formation pathways for clusters **2**–**4** by the reaction of $[Ru_3(CO)_{12}]$ with PH_2Mes. Formation of **1** can be rationalized by the coordination of mesitylphosphine and subsequent intramolecular oxidative addition of two P–H bonds accompanied by dissociation of overall three CO ligands [1]. After that, cluster **2** can produce under relatively mild conditions by a simple replacement of a CO ligand of **1** by the second mesitylphosphine. In refluxing toluene, **2** undergoes reductive elimination of H_2, intramolecular oxidative addition of two P–H bonds of the mesitylphosphine ligand, another reductive elimination of H_2, and final recoordination of a CO to afford cluster **3**. Then, **3** slowly reacts with $Ru(CO)_4$ generated from $Ru_3(CO)_{12}$ and subsequent dissociation of two CO ligands gives cluster **4**.

The molecular structures of complexes **1**–**5** were confirmed by X-ray crystallography. An ORTEP diagram of triruthenium complex **1** is shown in Fig. 1. Cluster **1** adopts a trigonal pyramidal geometry in which a μ_3-PMes ligand

caps a ruthenium triangle. Two hydrido ligands bridge over Ru(1)–Ru(2) and Ru(1)–Ru(3) bonds. These Ru–Ru bonds (Ru(1)–Ru(2) 2.9203(4) Å and Ru(1)–Ru(3) 2.9424(4) Å) are slightly longer than the Ru(2)–Ru(3) bond (2.7990(4) Å) that has no bridging hydrogen. Complex **1** is classified into a *nido*-type cluster with four vertices and is closely related to the known phosphinidene-bridged clusters $[Ru_3(CO)_9(\mu-H)_2(\mu_3-PR)]$ (R = Ph, *p*-$CH_3OC_6H_4$, Cy, etc.) [2b,2c,7]. In addition, the existence of equivalent two bridging hydrogen atoms were confirmed by the ^1H NMR spectrum, which shows a single resonance at -19.12 ppm as a doublet due to the coupling with the phosphorus atom of the phosphinidene ligand.

An ORTEP plot of **2** is exhibited in Fig. 2. A μ_3-PMes group caps the basal triangle composed of three ruthenium atoms, one of which is coordinated with a PH_2Mes ligand. The ^{31}P NMR spectrum shows the signals of μ_3-phosphinidene and terminal PH_2Mes ligands at moderately low field (233.6 ppm) and very high field (-99.2 ppm), respectively. In the ^1H NMR spectrum, the μ-hydride resonance
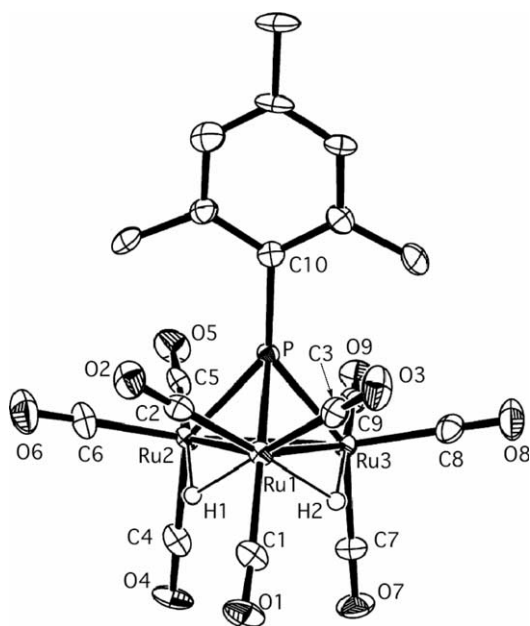

Fig. 1. Molecular structure of $[Ru_3(CO)_9(\mu-H)_2(\mu_3-PMes)]$ (**1**). Thermal ellipsoids are drawn at the 50% probability. Selected bond lengths (Å) and angles (°): Ru(1)–Ru(2) = 2.9426(4), Ru(1)–Ru(3) = 2.9207(4), Ru(2)–Ru(3) = 2.7993(4), Ru(1)–P = 2.3446(9), Ru(2)–P = 2.3240(9), Ru(3)–P = 2.3152(9); Ru(2)–Ru(1)–Ru(3) = 57.034(10), Ru(1)–Ru(2)–Ru(3) = 61.090(10), Ru(2)–Ru(3)–Ru(1) = 61.876(10), Ru(1)–P–Ru(2) = 78.14(3), Ru(1)–P–Ru(3) = 77.62(3), Ru(2)–P–Ru(3) = 74.23(3).
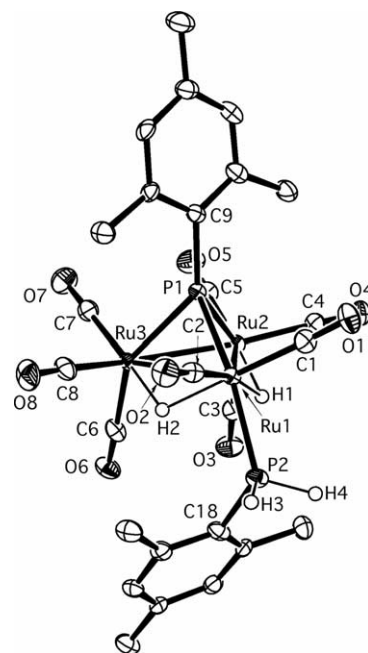

Fig. 2. Molecular structure of $[Ru_3(CO)_8(PH_2Mes)(\mu-H)_2(\mu_3-PMes)]$ (**2**). Thermal ellipsoids are drawn at the 50% probability. Selected bond lengths (Å) and angles (°): Ru(1)–Ru(2) = 2.9516(6), Ru(1)–Ru(3) = 2.9286(6), Ru(2)–Ru(3) = 2.7986(6), Ru(1)–P(1) = 2.3210(12), Ru(2)–P(1) = 2.3123(12), Ru(3)–P(1) = 2.3344(12), Ru(1)–P(2) = 2.3496(14); Ru(2)–Ru(1)–Ru(3) = 56.839(13), Ru(1)–Ru(2)–Ru(3) = 61.17(2), Ru(2)–Ru(3)–Ru(1) = 61.994(14), Ru(1)–P(1)–Ru(2) = 79.14(4), Ru(1)–P(1)–Ru(3) = 77.96(4), Ru(2)–P(1)–Ru(3) = 74.07(4), P(1)–Ru(1)–P(2) = 158.25(5), Ru(1)–P(2)–C(18) = 118.3(2).

of **2** appears at −18.89 ppm as a virtual triplet of triplet, coupled with two phosphorus nuclei (J_{PH} = 15.3 Hz) and two protons on the PH$_2$Mes ligand (J_{HH} = 1.8 Hz). Powell also reported the appearance of a triplet of triplet for the hydride signal of a related PPh complex [Ru$_3$(CO)$_8$(PH$_2$Ph)-(μ-H)$_2$(μ-PPh)] [8].

The molecular structure of complex **3** is depicted in Fig. 3. Complex **3** reveals a distorted square pyramidal geometry with the basal plane composed of two ruthenium and two phosphorus atoms, and a Ru(CO)$_3$ fragment at the apical position. Two aromatic rings of the mesityl groups are nearly coplanar to each other and adopt a twisted arrangement with respect to the basal plane. The Ru(1)–Ru(2) bond (2.9289(8) Å) is slightly longer than the Ru(1)–Ru(3) bond (2.8092(8) Å), probably due to the steric repulsion among two *o*-methyl groups (C(16) and C(27)) and carbonyl ligands on the Ru(1) and Ru(2) atoms. Such a steric repulsion can cause a restricted rotation of the mesityl groups, and indeed the ^{1}H NMR spectrum displays two resonances for inequivalent *o*-methyl groups at 2.67 and 2.68 ppm at room temperature.

Fig. 4 shows the molecular structure of tetraruthenium complex **4**. Cluster **4** has a *closo* octahedral framework. Both sides of the square Ru$_4$ plane are capped with two μ$_4$-phosphinidene ligands. Among eleven carbonyl groups, one (C(9)O(9)) bridges over the Ru(3)–Ru(4) bond, while the other ten carbonyl ligands are bound to the four ruthenium atoms in essentially terminal fashions. The IR spectrum clearly shows the existence of a bridging carbonyl with a v_{CO} band at 1809 cm^{-1} in addition to five v_{CO} bands for terminal carbonyl ligands. In more detailed analysis, two of the terminal carbonyl ligands (C(1)O(1) and C(4)O(4)) slightly tilt toward the adjacent ruthenium atoms (Ru(4) and Ru(3)) to take a semi bridging coordination mode. This geometry implies that the semi bridging CO ligands can easily migrate into the bridging positions. In fact, the ^{13}C NMR spectrum of **4** in CD$_2$Cl$_2$ shows only
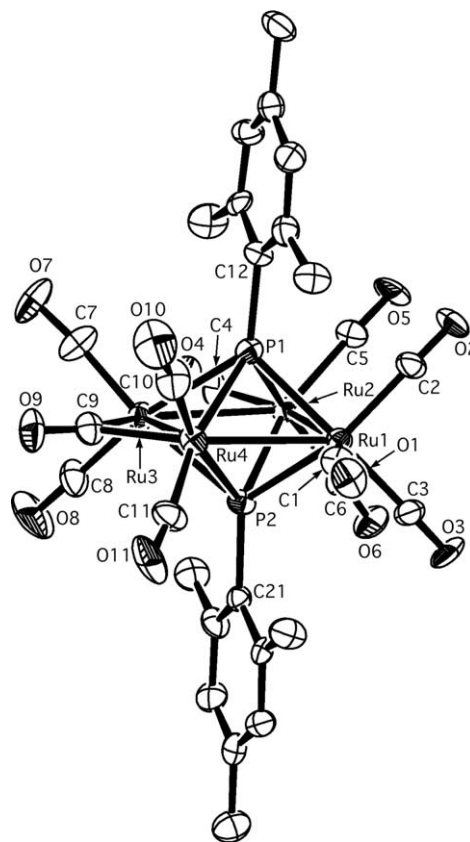

Fig. 4. Molecular structure of [Ru$_4$(CO)$_{10}$(μ-CO)(μ$_4$-PMes)$_2$] (**4**). Thermal ellipsoids are drawn at the 50% probability. Selected bond lengths (Å) and angles (°): Ru(1)–Ru(2) = 2.8092(8), Ru(2)–Ru(3) = 2.8976(8), Ru(3)–Ru(4) = 2.7107(8), Ru(4)–Ru(1) = 2.8976(8), Ru(1)–P(1) = 2.412(2), Ru(2)–P(1) = 2.416(2), Ru(3)–P(1) = 2.489(2), Ru(4)–P(1) = 2.548(2); Ru(1)–Ru(2)–Ru(3) = 89.00(2), Ru(2)–Ru(3)–Ru(4) = 90.95(2), Ru(1)–P(1)–Ru(2) = 71.16(6), Ru(1)–P(1)–Ru(4) = 71.44(5), Ru(3)–P(1)–Ru(4) = 65.11(5).

one broad signal at 202.3 ppm for the eleven CO ligands at room temperature. Thus, all carbonyl groups are exchanging their positions around the ruthenium four-membered ring
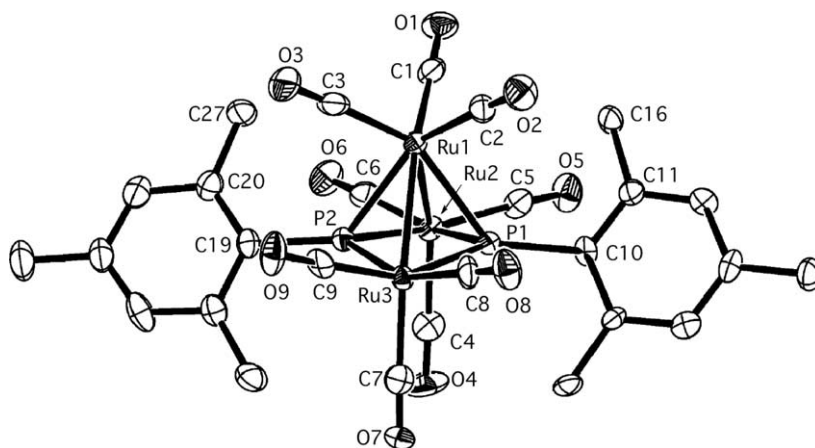

Fig. 3. Molecular structure of [Ru$_3$(CO)$_9$(μ$_3$-PMes)$_2$] (**3**). Thermal ellipsoids are drawn at the 50% probability. Selected bond lengths (Å) and angles (°): Ru(1)–Ru(2) = 2.9289(8), Ru(1)–Ru(3) = 2.8092(8), Ru(1)–P(1) = 2.370(2), Ru(2)–P(1) = 2.341(2), Ru(3)–P(1) = 2.357(2); Ru(2)–Ru(1)–Ru(3) = 82.09(2), Ru(2)–P(1)–Ru(3) = 106.71(7), Ru(2)–P(2)–Ru(3) = 106.31(7), P(1)–Ru(1)–P(2) = 71.34(6), P(1)–Ru(2)–P(2) = 72.70(6), P(1)–Ru(3)–P(2) = 71.95(6).

faster than the NMR time scale, probably with a merry-go-round process (Scheme 3) [3,9]. At −80 °C, the CO signal splits into four signals (δ 254.6, 201.0, 195.7, and 195.1 ppm) in the intensity ratio of 1:2:4:4. The same type of complex $[Ru_4(CO)_{10}(\mu\text{-}CO)(\mu_4\text{-}PPh)_2]$ reported by Smit et al. [3] also shows a fluxional behavior. But, in this compound, the scrambling of CO is so fast that the CO resonance does not decoalesce even at −114 °C. The slower CO scrambling observed in complex **4** is likely to be caused by the steric hindrance of bulky mesityl groups, which disturbs the merry-go-round process.
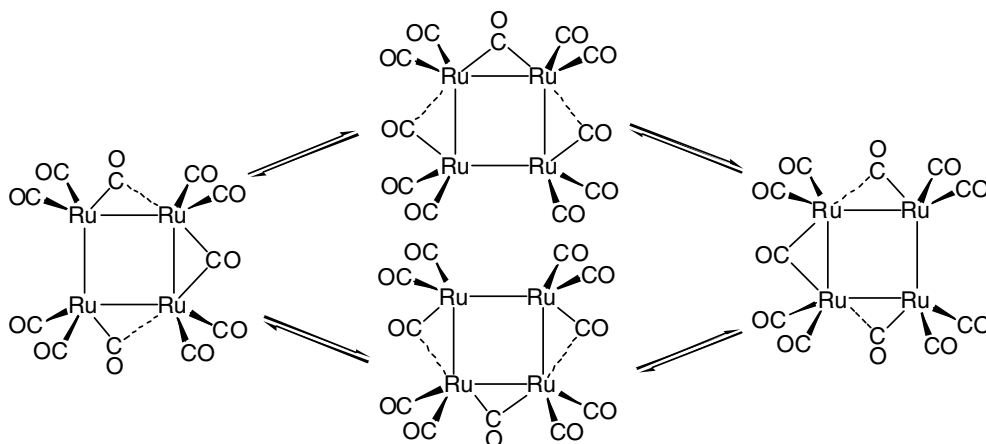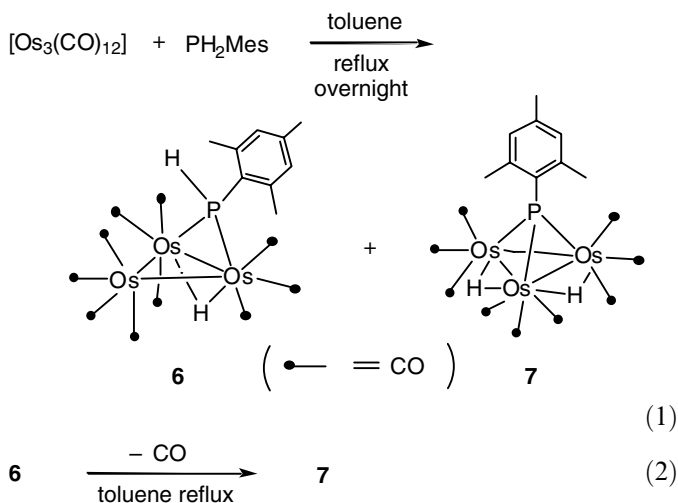
Fig. 5 depicts the result of X ray structural analysis of pentaruthenium cluster **5**. This compound has a bicapped-octahedral core. The five ruthenium atoms constitute a square pyramidal framework and each ruthenium atom bears two carbonyl ligands. The basal plane of the ruthenium pyramid is capped with a μ_4-PMes ligand, and two triangular faces are capped with μ_3-PMes units. In the pentaruthenium pyramid, Ru–Ru bonds from the apical Ru(1) atom to the four basal ruthenium atoms (2.8618(8)–2.9197(8) Å) are longer than the remaining Ru–Ru bonds in the basal plane (2.7915(8)–2.8896(8) Å). Although the positions of hydrido ligands attached to the ruthenium framework could not be determined in the crystal structural analysis, the existence of them were confirmed by ^{1}H NMR spectroscopy. A broad signal observed at −16.80 ppm (2H intensity) in the ^{1}H NMR spectrum clearly indicates that **5** has two bridging hydrido ligands. The ^{1}H NMR spectrum of **5** also shows two kinds of mesityl groups with an integral ratio of 2:1, which are in accord with the solid state structure of **5**.

A wide range of phosphinidene-bridged ruthenium carbonyl clusters has already been reported. Nonetheless, complex **5** is the first example of the phosphinidene-ruthenium cluster having a bicapped-octahedral skeletal framework. Related clusters reported previously are pseudo-octahedral pentaruthenium clusters, $[Ru_5(CO)_{15}(\mu_4\text{-}PPh)]$ and $[Ru_5(CO)_{13}(\mu_4\text{-}PPh)(\mu\text{-}PPh(OPr^n))(\mu\text{-}H)]$, and hexaruthenium clusters with a distorted trigonal prismatic

Ru$_6$ arrangement, $[Ru_6(CO)_{12}(\mu_4\text{-}PPh)_3(\mu_3\text{-}PPh)_2]$, $[Ru_6(CO)_{12}(\mu_4\text{-}PPh)_2(\mu_3\text{-}PPh)_2]$, $[Ru_6(CO)_{12}H_2(\mu_4\text{-}PPh)_2(\mu_3\text{-}PPh)_2]$, etc. [2,3,10]. Although the reaction pathway leading to cluster **5** is yet unexplainable, it is likely that sterically congested mesityl groups play a key role for the formation of its tightly closed novel framework.

2.2. Synthesis and structures of osmium clusters 6 and 7

In contrast to the ruthenium system, only two products were formed by the thermal reaction of $[Os_3(CO)_{12}]$ with PH_2Mes in refluxing toluene. Triosmium complexes $[Os_3(CO)_{10}(\mu\text{-}H)(\mu\text{-}PHMes)]$ (**6**) and $[Os_3(CO)_9(\mu\text{-}H)_2(\mu_3\text{-}PMes)]$ (**7**) were obtained in 19% and 40% yields, respectively (Eq. (1)). Wheatley et al. [2b] have reported a similar thermal reaction between $[Os_3(CO)_{12}]$ and PH_2Ph producing the phenyl-substituted derivatives, $[Os_3(CO)_{10}(\mu\text{-}H)(\mu\text{-}PHPh)]$ and $[Os_3(CO)_9(\mu\text{-}H)_2(\mu_3\text{-}PPh)]$. They described that phosphido-bridged complex $[Os_3(CO)_{10}(\mu\text{-}H)(\mu\text{-}PHPh)]$ transformed into phosphinidene-capped cluster $[Os_3(CO)_9(\mu\text{-}H)_2(\mu_3\text{-}PPh)]$ via loss of CO ligand on heating. Similar to this, refluxing of a toluene solution of **6** gave **7** in 84% yield (Eq. (2)).

$$[Os_3(CO)_{12}] + PH_2Mes \xrightarrow[\text{reflux overnight}]{\text{toluene}}$$

6 + **7** $\qquad (\longleftarrow = CO)$

(1)

$$\textbf{6} \xrightarrow[\text{toluene reflux}]{-\ CO} \textbf{7}$$

(2)

Scheme 3. A plausible exchange process (merry-go-round process) of carbonyl groups in complex **4** (phosphinidene unites are omitted for clarity).
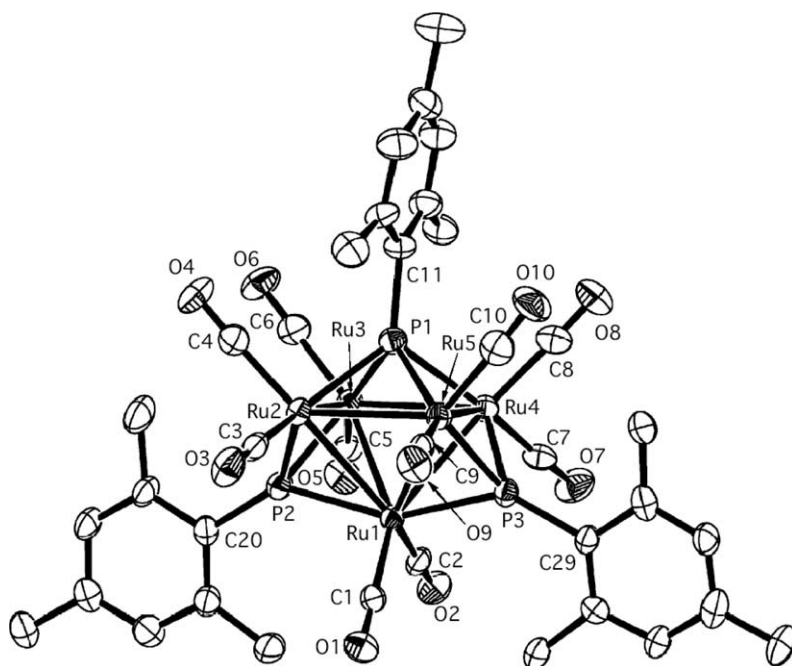
Fig. 5. Molecular structure of [Ru$_5$(CO)$_{10}$H$_2$(μ_4-PMes)(μ_3-PMes)$_2$] (**5**). Thermal ellipsoids are drawn at the 50% probability. Selected bond lengths (Å) and angles (°): Ru(1)–Ru(2) = 2.9197(8), Ru(1)–Ru(3) = 2.8681(8), Ru(1)–Ru(4) = 2.8913(8), Ru(1)–Ru(5) = 2.9163(8), Ru(2)–Ru(3) = 2.8308(8), Ru(3)–Ru(4) = 2.7915(8), Ru(4)–Ru(5) = 2.8296(8), Ru(2)–Ru(5) = 2.8896(8), Ru(1)–P(2) = 2.399(2), Ru(2)–P(2) = 2.272(2), Ru(2)–P(1) = 2.388(2); Ru(1)–Ru(2)–Ru(3) = 59.81(2), Ru(1)–Ru(2)–Ru(5) = 60.26(2), Ru(2)–Ru(1)–Ru(3) = 58.56(2), Ru(2)–Ru(1)–Ru(5) = 59.36(2), Ru(2)–Ru(1)–Ru(4) = 87.31(2), Ru(2)–Ru(3)–Ru(4) = 91.04(2), Ru(1)–P(2)–Ru(2) = 77.31(6), Ru(2)–P(2)–Ru(3) = 76.78(6), Ru(2)–P(1)–Ru(3) = 71.87(6), Ru(2)–P(1)–Ru(5) = 74.38(6).

The X-ray crystal structures of **6** and **7** are depicted in Figs. 6 and 7, respectively. Their structures closely resemble those of the phenyl-substituted clusters [Os$_3$(CO)$_{10}$(μ-H)(μ-PHPh)]

and [Os$_3$(CO)$_9$(μ-H)$_2$(μ_3-PPh)], respectively. In complex **6**, one Os–Os edge of the osmium triangle is bridged by μ-phosphido and μ-hydrido ligands. The Os–Os bond bridged by
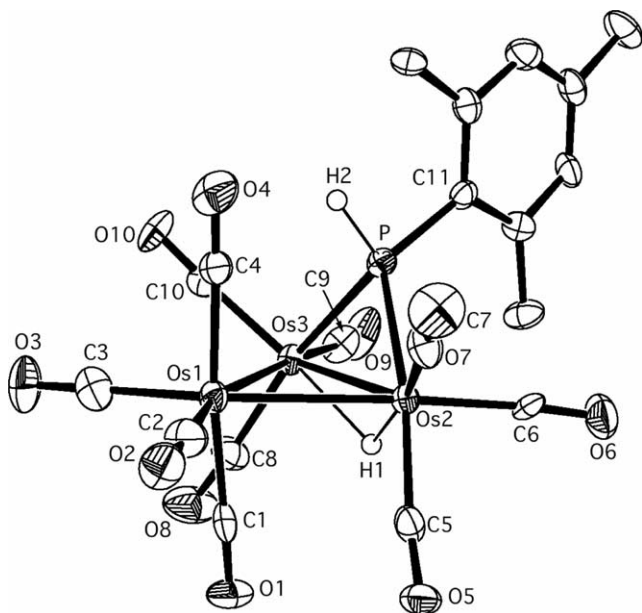

Fig. 6. Molecular structure of [Os$_3$(CO)$_{10}$(μ-H)(μ-PHMes)] (**6**). Thermal ellipsoids are drawn at the 50% probability. Selected bond lengths (Å) and angles (°): Os(1)–Os(2) = 2.8879(6), Os(1)–Os(3) = 2.8983(6), Os(2)–Os(3) = 2.9387(6), Os(2)–P = 2.377(3), Os(3)–P = 2.383(3); Os(2)–Os(1)–Os(3) = 61.046(14), Os(1)–Os(2)–Os(3) = 59.65(2), Os(2)–Os(3)–Os(1) = 59.303(14), Os(2)–P–Os(3) = 76.25(8), P–Os(2)–Os(1) = 84.38(7), P–Os(2)–Os(3) = 51.97(7), P–Os(3)–Os(1) = 84.04(6), P–Os(3)–Os(2) = 51.78(7).
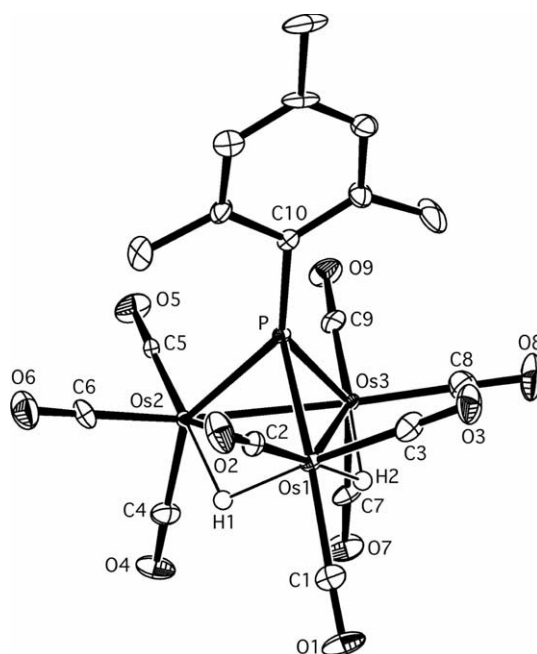

Fig. 7. Molecular structure of [Os$_3$(CO)$_9$(μ-H)$_2$(μ_3-PMes)] (**7**). Thermal ellipsoids are drawn at the 50% probability. Selected bond lengths (Å) and angles (°): Os(1)–Os(2) = 2.9647(5), Os(1)–Os(3) = 2.9478(5), Os(2)–Os(3) = 2.8240(5), Os(1)–P = 2.369(2), Os(2)–P = 2.347(2), Os(3)–P = 2.342(2); Os(2)–Os(1)–Os(3) = 57.060(12), Os(1)–Os(2)–Os(3) = 61.168(12), Os(2)–Os(3)–Os(1) = 61.772(12), Os(1)–P–Os(2) = 77.89(6), Os(1)–P–Os(3) = 77.46(6), Os(2)–P–Os(3) = 74.06(6).

these ligands, i.e., Os(2)–Os(3) (2.9387(6) Å), is slightly longer than the other two Os–Os bonds (Os(1)–Os(2); 2.8879(6) and Os(1)–Os(3); 2.8983(6) Å, respectively). The ^{1}H NMR spectrum of **6** shows the μ-hydrido signal at −18.61 ppm as a doublet of doublet coupled with the phosphorus atom (J_{PH} = 19.0 Hz) and PH proton (J_{HH} = 4.5 Hz). The proton on the μ-phosphido ligand resonates at the characteristic low field, 7.82 ppm, as a doublet of doublet (J_{PH} = 413.4 Hz, J_{HH} = 4.5 Hz).

Cluster **7** is virtually isostructural with its ruthenium analogue **1**. The mesitylphosphinidene ligand caps the basal metal triangle and two hydride ligands bridge over two of the Os–Os edges. In the osmium triangle, the bond lengths between Os(1)–Os(2) and Os(1)–Os(3) (2.9681(5) and 2.9585(5) Å, respectively), which were bridged by the hydrido ligands, are slightly longer than that of Os(2)–Os(3) (2.8243(5) Å); the same tendency was also found in the ruthenium analogue **1**. The ^{1}H NMR spectrum displays the μ-hydrido resonance at −20.84 ppm as a doublet coupled with the phosphorus atom.

3. Conclusion

Mesitylphosphinidene-capped tri, tetra, and pentaruthenium clusters **1**–**5** were synthesized by the thermal reaction of [$Ru_3(CO)_{12}$] with PH_2Mes and structurally characterized. Clusters **2**–**4** were obtained selectively in high yields by stepwise reactions starting from **1**. In the case of [$Ru_4(CO)_{10}$(μ-CO)(μ$_4$-PMes)$_2$] (**4**), fluxional behavior involving the migration of all carbonyl groups around tetraruthenium atoms was observed. [$Ru_5(CO)_{10}H_2$(μ$_4$-PMes)(μ$_3$-PMes)$_2$] (**5**) has a novel bicapped-octahedral framework in which a square pyramidal core composed of five $Ru(CO)_2$ fragments is capped with one μ$_4$- and two μ$_3$-mesitylphosphinidene units. Although the reaction pathway for **5** is not clarified yet, bulky mesityl group is likely to play an important role for the formation of its tightly closed skeletal framework. In contrast with the ruthenium system, the thermal reaction of [$Os_3(CO)_{12}$] with PH_2Mes exclusively afforded trinuclear complexes, i.e., phosphido-bridged complex [$Os_3(CO)_{10}$(μ-H)(μ-PHMes)] (**6**) and mesitylphosphinidene-capped cluster [$Os_3(CO)_9$(μ-H)$_2$(μ$_3$-PMes)] (**7**).

4. Experimental

4.1. General procedure

All reactions were performed under dry nitrogen atmosphere, using standard Schlenk techniques. Toluene and hexane were distilled from sodium-benzophenone ketyl just before use. Dichloromethane was dried over calcium hydride and purified by trap-to-trap distillation. ^{1}H, ^{13}C, and ^{31}P NMR spectra were recorded on a Bruker ARX 300 spectrometer or a Bruker AVANCE 300 instrument. ^{1}H and ^{13}C NMR chemical shifts were referenced to SiMe$_4$ as the standard (δ = 0). ^{31}P NMR chemical shifts were ref-

erenced to an 85% H_3PO_4 used as an external standard. IR spectra were measured on a HORIBA FT-730 spectrometer. Elemental analyses were performed at the Instrumental Analysis Center for Chemistry, Tohoku University. Mesitylphosphine were prepared according to the literature method [11]. All other reagents were purchased and used without further purification.

4.2. Reaction of [$Ru_3(CO)_{12}$] and PH_2Mes

(a) A toluene (25 mL) solution of [$Ru_3(CO)_{12}$] (300 mg, 0.469 mmol) and PH_2Mes (71 mg, 0.47 mmol) was refluxed for 30 min. The color of the solution changed from orange to red during the reaction. The reaction mixture was filtered and celite (ca. 1 g) was added to the filtrate to adsorb the products. After removal of solvent under reduced pressure, the celite was subjected to a silica gel flash column (3 × 10 cm). Initially, hexane was used to elute a known orange complex [Ru_4(μ-H)$_4$(CO)$_{12}$] (50 mg), and following three yellow fractions. Concentration of the yellow fractions gave [$Ru_3(CO)_9$(μ-H)$_2$(μ$_3$-PMes)] (**1**) (88 mg, 0.12 mmol, 27%), [$Ru_3(CO)_9$(μ$_3$-PMes)$_2$] (**3**) (30 mg, 0.035 mmol, 15%), and [$Ru_3(CO)_8$(PH_2Mes)(μ-H)$_2$(μ$_3$-PMes)] (**2**) (15 mg, 0.018 mmol, 7.7%), respectively. Subsequently hexane–toluene mixtures with increasing toluene content (up to 4:1 ratio) were used to elute the forth and fifth fractions colored red and violet, respectively. Concentration of the red fraction and violet fraction afforded [$Ru_5(CO)_{10}H_2$(μ$_4$-PMes)(μ$_3$-PMes)$_2$] (**5**) (32 mg, 0.026 mmol, 17%) and [$Ru_4(CO)_{10}$(μ-CO)(μ$_4$-PMes)$_2$] (**4**) (5 mg, 0.005 mmol, 2% yield), respectively.

1: yellow platelets. ^{1}H NMR (300 MHz, CD$_2$Cl$_2$): δ −19.12 (d, $^2J_{PH}$ = 15.0 Hz, 2H, μ-H), 2.03 (s, 3H, p-CH$_3$), 2.44 (s, 6H, o-CH$_3$), 6.75 (d, $^4J_{PH}$ = 3.6 Hz, 2H, ArH). ^{31}P NMR (121.5 MHz, CD$_2$Cl$_2$): δ 218.8 (t, J_{PH} = 15.0 Hz). ^{13}C NMR (75.5 MHz, CD$_2$Cl$_2$): δ 21.2 (s, p-CH$_3$), 26.7 (d, J_{pc} = 12.1 Hz, o-CH$_3$), 128.4 (d, J_{pc} = 19.6 Hz, ipso-$C_6H_2Me_3$), 132.2 (d, J_{pc} = 9.1 Hz, o-$C_6H_2Me_3$), 141.7 (d, J_{pc} = 3.8 Hz, p-$C_6H_2Me_3$), 142.8 (d, J_{pc} = 9.1 Hz, m-$C_6H_2Me_3$), 190.9, 198.0 (br, CO). IR ν_{CO} (KBr, cm^{-1}): 2106 (m), 2071 (s), 2042 (vs), 2005 (s), 1996(s), 1976(s). Anal. Calc. for C$_{18}$H$_{13}$O$_9$PRu$_3$: C, 30.56; H, 1.85. Found: C, 30.93; H, 2.01.

2: yellow prisms. ^{1}H NMR (300 MHz, CD$_2$Cl$_2$): δ −18.89 (tt, 2H, $^2J_{PH}$ = 15.3 Hz, $^3J_{HH}$ = 1.8 Hz, μ-H), 2.09 (s, 3H, p-CH$_3$), 2.20 (s, 3H, p-CH$_3$), 2.36 (s, 6H, o-CH$_3$), 2.66 (s, 6H, o-CH$_3$), 5.67 (dm, 2H, $^1J_{PH}$ = 355.2 Hz, PH), 6.88 (d, 2H, $^4J_{PH}$ = 3.6 Hz, ArH), 6.94 (d, 2H, $^4J_{PH}$ = 3.6 Hz, ArH). ^{31}P NMR (121.5 MHz, CD$_2$Cl$_2$): δ 233.6 (dt, J_{PP} = 113.6 Hz, J_{PH} = 15.3 Hz, μ-PMes), −99.2 (dtt, J_{PH} = 355.2 Hz, J_{PP} = 113.6 Hz, J_{PH} = 15.3 Hz, PH_2Mes). ^{13}C NMR (75.5 MHz, CD$_2$Cl$_2$): δ 21.1 (d, J_{pc} = 4.5 Hz), 21.7 (s), 21.8 (s), 26.6 (d, J_{pc} = 11.3 Hz) (all for Me), 121.2 (s), 121.9 (s), 129.9 (d, J_{pc} = 7.6 Hz), 130.8 (d, J_{pc} = 8.3 Hz), 131.3 (s), 139.7 (d, J_{pc} = 8.3 Hz), 140.9 (br, m), 142.4 (d, J_{pc} = 9.1 Hz) (all for Ph), 191.0 (m), 196.6 (m), 200.5 (br), 201.1 (br) (all for CO). IR ν_{CO}

(KBr, cm^{-1}): 2071 (m), 2032 (vs), 2009 (s), 1993 (s), 1973 (s) 1957 (s). Anal. Calc. for $C_{26}H_{26}O_8P_2Ru_3$: C, 37.55; H, 3.15. Found: C, 37.05; H, 3.38.

3: yellow prisms. ^{1}H NMR (300 MHz, CD$_2$Cl$_2$): δ 2.20 (s, 6H, *p*-CH$_3$), 2.67 (s, 6H, *o*-CH$_3$), 2.68 (s, 6H, *o*-CH$_3$), 6.87 (s, 2H, ArH), 6.88 (s, 2H, ArH). ^{31}P NMR (121.5 MHz, CD$_2$Cl$_2$): δ 184.2 (s). ^{13}C NMR (75.5 MHz, CD$_2$Cl$_2$): δ 21.0 (s), 23.1 (br) 27.2 (t, J_{pc} = 6.8 Hz) (all for Me), 129.8 (br), 130.6 (br), 132.4 (s), 139.6 (s), 140.3 (t, J_{pc} = 7.6 Hz), 140.7 (br) (all for Ph), 193.3 (t, J_{pc} = 28.7 Hz), 199.6 (s), 200.8 (t, J_{pc} = 9.8 Hz) (all for CO). IR v_{CO} (KBr, cm^{-1}): 2060 (s), 2048 (s), 2036 (s), 2009 (s), 1998 (vs), 1961(m). Anal. Calc. for $C_{27}H_{22}O_9P_2Ru_3$: C, 37.90; H, 2.59. Found: C, 38.08; H, 2.35.

4: violet prisms. ^{1}H NMR (300 MHz, CD$_2$Cl$_2$): δ 2.02 (s, 6H, *p*-CH$_3$), 2.26 (s, 12H, *o*-CH$_3$), 6.60 (s, 4H, ArH). ^{31}P NMR (121.5 MHz, CD$_2$Cl$_2$): δ 151.2 (s). ^{13}C NMR (75.5 MHz, CD$_2$Cl$_2$ at 296 K): δ 20.7 (s, *p*-CH$_3$), 24.0 (t, J_{PC} = 6.0 Hz, *o*-CH$_3$), 124.6 (t, J_{PC} = 13.4 Hz, *ipso*-C$_6$H$_2$Me$_3$), 130.9 (t, J_{PC} = 3.8 Hz, *m*-C$_6$H$_2$Me$_3$), 140.2 (t, J_{PC} = 4.5 Hz, *o*-C$_6$H$_2$Me$_3$), 141.2 (s, *p*-C$_6$H$_2$Me$_3$), 202.3 (br, CO); (at 193 K) 195.1 (br, CO), 195.7 (br, CO), 201.0 (br, CO), 254.6 (br, μ-CO). IR v_{CO} (KBr, cm^{-1}): 2075 (w), 2041 (s), 2026 (vs), 2006 (s), 1959 (s), 1809 (s). Anal. Calc. for $C_{29}H_{22}O_{11}P_3Ru_4$: C, 34.39; H, 2.19. Found: C, 34.45; H, 2.38.

5: red platelets. ^{1}H NMR (300 MHz, CD$_2$Cl$_2$): δ −16.80 (br s, 2H, μ-H), 2.12 (s, 3H, *p*-CH$_3$ of μ_4-PMes), 2.30 (s, 6H, *p*-CH$_3$ of μ_3-PMes), 2.68 (s, 12H, *o*-CH$_3$ of μ_4-PMes), 2.79 (s, 6H, *o*-CH$_3$ of μ_3-PMes), 6.80 (br s, 2H, μ_4-PC$_6$H$_2$Me$_3$), 7.03 (br s, 6H, μ_3-PC$_6$H$_2$Me$_3$). ^{31}P NMR (121.5 MHz, CD$_2$Cl$_2$): δ 447.4–450.3 (m, μ-P). ^{13}C NMR (75.5 MHz, CD$_2$Cl$_2$): δ 21.1 (s), 21.3 (s), 25.9 (d, J_{pc} = 5.3 Hz), 29.7 (d, J_{pc} = 14.3 Hz) (all for Me), 131.1 (m), 131.8 (m), 139.3 (m), 141.2 (m), 141.8 (s), 142.2 (s), 143.45 (s) (all for Ph), 192.3 (br), 200.3 (br), 200.7 (br) (all for CO). IR v_{CO} (KBr, cm^{-1}): 2030 (s), 2019 (s), 2009 (vs), 1999 (s), 1972 (s), 1957 (m). Anal. Calc. for $C_{37}H_{35}O_{10}P_3Ru_5$: C, 35.90; H, 2.85. Found: C, 36.19; H, 3.19.

(b) A toluene (40 mL) solution of PH$_2$Mes (142 mg, 0.933 mmol) and [Ru$_3$(CO)$_3$] (600 mg, 0.969 mmol) was refluxed overnight. The color of the solution changed from orange to dark brown. Chromatographic separation of the resulting mixture in a manner analogous to that described in (a) yielded [Ru$_4$(μ-H)$_4$(CO)$_{12}$] (39 mg), **1** (169 mg, 0.237 mmol, 25.5%), **3** (54 mg, 0.064 mmol, 14%), **5** (118 mg, 0.0956 mmol, 30.7%), and **4** (48 mg, 0.048 mmol, 10%), in this order.

(c) When a toluene (10 mL) solution of [Ru$_3$(CO)$_{12}$] (200 mg, 0.313 mmol) and twofold excess PH$_2$Mes (98 mg, 0.64 mmol) was refluxed overnight and worked up as above, [Ru$_4$(μ-H)$_4$(CO)$_{12}$] (10 mg), **1** (54 mg, 0.077 mmol, 12%), **3** (13 mg, 0.042 mmol, 13%), **5** (87 mg, 0.070 mmol, 33%), and **4** (23 mg, 0.023 mmol, 7.1%) were obtained. Under this condition, three kinds of brown oily products (11, 15, and 15 mg) were obtained after compound **4** was eluted, but they could not be identified.

(d) When the reaction of [Ru$_3$(CO)$_{12}$] (200 mg, 0.312 mmol) with PH$_2$Mes (49 mg, 0.32 mmol) was performed in hexane (30 mL) under reflux overnight, a dark orange solution was produced. The solution was worked up by the procedure similar to that described in (a) to afford [Ru$_4$(μ-H)$_4$(CO)$_{12}$] (52 mg), **1** (25 mg, 0.036 mmol, 11%), **3** (11 mg, 0.013 mmol, 7.8%), **2**, (38 mg, 0.046 mmol, 29%), **5** (6 mg, 0.005 mmol, 5%), and **4** (7 mg, 0.007 mmol, 4%), in this order.

4.3. Reaction of [Ru$_3$(CO)$_9$(μ-H)$_2$(μ_3-PMes)] (1) with PH$_2$Mes

A hexane solution (15 mL) of [Ru$_3$(CO)$_9$(μ-H)$_2$(μ_3-PMes)] (**1**) (33 mg, 0.047 mmol) and PH$_2$Mes (10 mg, 0.066 mmol) was heated under reflux overnight. The yellow solution was adsorbed on celite, and the solvent was removed under reduced pressure. Flash chromatography (hexane/toluene (5:1)) on silica gel (2 × 4 cm) gave a single product characterized as [Ru$_3$(CO)$_8$(PH$_2$Mes)(μ-H)$_2$(μ_3-PMes)] (**2**) (30 mg, 0.036 mmol, 78%).

4.4. Reaction of [Ru$_3$(CO)$_8$(PH$_2$Mes)(μ-H)$_2$(μ_3-PMes)] (2) with carbon monoxide

A toluene solution (20 mL) of [Ru$_3$(CO)$_8$(PH$_2$Mes)(μ-H)$_2$(μ_3-PMes)] (**2**) (30 mg, 0.036 mmol) were refluxed for 3 h under carbon monoxide atmosphere. The brown solution was adsorbed on celite, and the solvent was removed under reduced pressure. Flash chromatography (hexane/toluene (5:1)) on silica gel (2 × 4 cm) gave [Ru$_3$(CO)$_9$(μ_3-PMes)$_2$] (**3**) (17 mg, 0.020 mmol, 56%) from the first yellow band. The second red band and third brown band afforded unidentified powders (4 mg and 6 mg, respectively) after evaporation.

4.5. Reaction of [Ru$_3$(CO)$_9$(μ_3-PMes)$_2$] (3) with [Ru$_3$(CO)$_{12}$]

A toluene solution (3 mL) of [Ru$_3$(CO)$_9$(μ_3-PMes)$_2$] (**3**) (12 mg, 0.014 mmol) and [Ru$_3$(CO)$_{12}$] (9 mg, 0.014 mmol) was stirred under reflux for 2 days. Celite was added to the reaction mixture, and solvent was removed under reduced pressure. The celite was then subjected to a silica gel flash column (2 × 10 cm). Elution with hexane/toluene (4:1) afforded [Ru$_3$(CO)$_{12}$] (1 mg) as a first yellow band. The second brown band and the third red-brown band yielded unidentified powders (2 mg and 1 mg, respectively) after evaporation. From the forth violet band, [Ru$_4$(CO)$_{10}$(μ-CO)(μ_4-PMes)$_2$] (**4**) (11 mg, 0.011 mmol, 78%) was obtained as violet crystals.

4.6. Reaction of [Os$_3$(CO)$_{12}$] with PH$_2$Mes

A toluene solution of [Os$_3$(CO)$_{12}$] (150 mg, 0.165 mmol) and PH$_2$Mes (25 mg, 0.16 mmol) was refluxed overnight. The resulting mixture was filtered and to the filtrate was

Table 1
Crystal data and structure refinements of **1**–**7**

	1	**2**	**3**	**4**	**5**	**6**	**7**
Crystal size (mm)	$0.20 \times 0.10 \times 0.10$	$0.50 \times 0.10 \times 0.10$	$0.10 \times 0.10 \times 0.05$	$0.10 \times 0.05 \times 0.05$	$0.20 \times 0.15 \times 0.10$	$0.10 \times 0.10 \times 0.10$	$0.30 \times 0.20 \times 0.10$
Formula	$C_{18}H_{13}O_9PRu_3$	$C_{26}H_{26}O_8P_2Ru_3$	$C_{27}H_{22}O_9P_2Ru_3$	$C_{29}H_{22}O_{11}P_2Ru_4$	$C_{37}H_{35}O_{10}P_3Ru_5$	$C_{19}H_{13}O_{10}Os_3P$	$C_{18}H_{13}O_9Os_3P$
F_w	707.46	831.62	855.60	1012.69	1237.91	1002.86	974.85
Crystal system	$P\bar{1}$	$P\bar{1}$	$Pbca$	$P2_12_12_1$	$P\bar{1}$	$P2_1$	$P\bar{1}$
Space group	Triclinic	Triclinic	Orthorhombic	Orthorhombic	Triclinic	Monoclinic	Triclinic
a (Å)	8.3391(3)	8.7796(13)	8.9384(6)	12.4760(7)	12.3724(9)	9.3882(10)	8.3506(6)
b (Å)	9.2269(6)	11.070(2)	17.9644(14)	12.4760(7)	16.8044(8)	8.9896(7)	9.1801(6)
c (Å)	16.5936(10)	16.598(2)	37.794(2)	21.4411(8)	23.8596(11)	14.5184(14)	16.5294(11)
α (°)	90.135(2)	106.435(7)			98.758(2)		89.971(3)
β (°)	102.922(2)	103.563(6)			102.732(5)	99.804(5)	76.807(4)
γ (°)	114.998(2)	94.346(4)			105.908(2)		65.370(2)
Volume (Å^3)	1121.1(1)	1486.6(4)	6068.6(7)	3337.3(3)	4532.2(4)	1207.4(2)	1115.02(13)
Z	2	2	8	4	4	2	2
ρ_{calc} (g cm^{-3})	2.096	1.858	1.873	2.016	1.814	2.758	2.904
μ (mm^{-1})	2.112	1.657	1.629	1.928	1.783	15.862	17.169
$F(000)$	680	816	3344	1960	2408	900	872
Reflections collected	10721	13260	44160	28534	38228	10173	10058
Independent reflections	5077 [R(int) = 0.0188]	6645 [R(int) = 0.0359]	6832 [R(int) = 0.0989]	7593 [R(int) = 0.0628]	19594 [R(int) = 0.0461]	5179 [R(int) = 0.0440]	4849 [R(int) = 0.0442]
Max. and min. transmission	0.8166 and 0.6774	0.8518 and 0.4913	0.9230 and 0.8541	0.9098 and 0.8306	0.8418 and 0.7169	0.2999 and 0.2999	0.2786 and 0.0791
Data/restrains/parameters	5077/0/291	6645/0/374	6832/0/376	7593/0/421	19594/0/1009	5179/0/309	4849/0/290
GOF on F^2	1.295	1.164	1.238	1.264	1.095	1.069	1.269
Final R indices [$I > 2\sigma(I)$]	$R_1 = 0.0216$, $wR_2 = 0.0736$	$R_1 = 0.0420$, $wR_2 = 0.1324$	$R_1 = 0.0743$, $wR_2 = 0.1392$	$R_1 = 0.0422$, $wR_2 = 0.1024$	$R_1 = 0.0600$, $wR_2 = 0.1809$	$R_1 = 0.0397$, $wR_2 = 0.1116$	$R_1 = 0.0382$, $wR_2 = 0.1122$
R indices (all data)	$R_1 = 0.0249$, $wR_2 = 0.0961$	$R_1 = 0.0496$, $wR_2 = 0.1789$	$R_1 = 0.0891$, $wR_2 = 0.1622$	$R_1 = 0.0513$, $wR_2 = 0.1158$	$R_1 = 0.0731$, $wR_2 = 0.1998$	$R_1 = 0.0407$, $wR_2 = 0.1154$	$R_1 = 0.0394$, $wR_2 = 0.1130$
Largest diff. peak and hole (e Å^{-3})	0.785 and −1.088	1.295 and −3.904	1.384 and −1.632	0.919 and −1.073	3.648 and −2.321	1.371 and −2.843	1.643 and −3.523

added celite. After removal of solvent, the celite was subjected to a silica gel flash column (3×20 cm) and chromatographed with a hexane/toluene (10:1) mixture. The first yellow fraction was evaporated to afford $[Os_3(CO)_{10}(\mu\text{-H})(\mu\text{-PHMes})]$ (**6**) (31 mg, 0.031 mmol, 19%) and the second pale yellow fraction gave $[Os_3(CO)_9(\mu\text{-H})_2(\mu_3\text{-PMes})]$ (**7**) (63 mg, 0.065 mmol, 40%).

6: yellow platelets. ^{1}H NMR (300 MHz, CD_2Cl_2): δ −18.61 (dd, 1H, $^2J_{PH} = 19.0$ Hz, $^3J_{HH} = 4.5$ Hz, μ-H), 2.16 (s, 3H, p-CH$_3$), 2.42 (s, 6H, o-CH$_3$), 6.81 (d, 2H, $^4J_{PH} = 3.6$ Hz, ArH), 7.82 (dd, 1H, $^1J_{PH} = 413.4$ Hz, $^3J_{HH} = 4.5$ Hz, μ-PH). ^{31}P NMR (121.5 MHz, CD_2Cl_2): δ −84.6 (dd, $J_{PH} = 413.4$ Hz, $J_{PH} = 19.0$ Hz). ^{13}C NMR (75.5 MHz, CD_2Cl_2): δ 21.0 (s, p-CH$_3$), 24.5 (d, $J_{PC} = 11.3$ Hz, o-CH$_3$), 125.7 (d, $J_{PC} = 47.5$ Hz, $ipso$-$C_6H_2Me_3$), 131.1 (d, $J_{PC} = 9.06$ Hz, m-$C_6H_2Me_3$), 140.4 (s, o-$C_6H_2Me_3$), 141.6 (d, $J_{PC} = 9.1$ Hz, p-$C_6H_2Me_3$), 170.8 (d, $J_{PC} = 9.1$ Hz), 173.7 (s), 173.6. (d, $J_{PC} = 9.1$ Hz), 177.7 (s), 178.5 (s), 180.9 (d, $J_{PC} = 10.3$ Hz), 185.0 (d, $J_{PC} = 20.7$ Hz) (all for CO). IR ν_{CO} (KBr, cm^{-1}): 2101 (s), 2056 (vs), 2047 (vs), 2032 (m), 2015 (m) 1997 (s), 1985 (s), 1970 (s). Anal. Calc. for $C_{18}H_{13}O_9Os_3P$: C, 22.75; H, 1.31, Found: C, 22.83; H, 1.32.

7: pale yellow prisms. ^{1}H NMR (300 MHz, CD_2Cl_2): δ −20.84 (d, 2H, $^2J_{PH} = 9.9$ Hz, μ-H), 2.23 (s, 3H, p-CH$_3$), 2.65 (s, 6H, o-CH$_3$), 6.97 (d, 2H, $^4J_{PH} = 4.5$ Hz, ArH). ^{31}P NMR (121.5 MHz, CD_2Cl_2): δ 53.6 (br, m). ^{13}C NMR (75.5 MHz, CD_2Cl_2): δ 21.2 (s, p-CH$_3$), 27.0 (d, $J_{PC} = 12.8$ Hz, o-CH$_3$), 119.8 (d, $J_{PC} = 18.1$ Hz, $ipso$-$C_6H_2Me_3$), 130.6 (d, $J_{PC} = 9.1$ Hz, m-$C_6H_2Me_3$), 141.3 (d, $J_{PC} = 3.8$ Hz, p-$C_6H_2Me_3$), 142.9 (d, $J_{PC} = 9.8$ Hz, o-$C_6H_2Me_3$), 155.5 (br), 162.1 (br), 169.4 (br), 171.9 (br), 176.6 (br) (all for CO). IR ν_{CO} (KBr, cm^{-1}): 2104 (s), 2071 (s), 2039 (vs), 2018 (s), 1996 (s), 1983 (s), 1968 (s). Anal. Calc. for $C_{18}H_{13}O_9Os_3P$: C, 22.17; H, 1.34, Found: C, 22.22; H, 1.33.

4.7. Thermolysis of $[Os_3(CO)_{10}(\mu\text{-H})(\mu\text{-PHMes})]$ (6)

A solution of complex $[Os_3(CO)_{10}(\mu\text{-H})(\mu\text{-PHMes})]$ (**6**) (22 mg, 0.022 mmol) in toluene (8 mL) was heated under reflux overnight. The solution was filtered and the solvent was removed under vacuum. Recrystallization from hexane at −30 °C gave microcrystalline solid of $[Os_3(CO)_9(\mu\text{-H})_2(\mu_3\text{-PMes})]$ (**7**) (18 mg, 0.019 mmol, 84%).

4.8. X-ray diffraction analysis

Single crystals of **1**, **2**, **3**, **4**, and **5** suitable for X-ray diffraction analysis were obtained by cooling their toluene solutions layered with hexane at −30 °C. Crystals of **6** and **7** were grown from the CH$_2$Cl$_2$ solutions layered with hexane at room temperature. Intensity data were collected on a RIGAKU RAXIS-RAPID Imaging Plate diffractometer with graphite monochromated Mo Kα radiation at 150 K. The data were corrected for Lorentz and polarization effects and numerical absorption corrections were

applied. The crystallographic data are listed in Table 1. The structures were solved by Patterson and Fourier synthesis methods using SHELXS-97 [12] and refined by full matrix least-squares techniques on all F^2 data. In complexes **1**–**4**, **6**, and **7**, the hydrogen atoms bridging Ru–Ru or Os–Os bonds and on the phosphorus atoms were located by the differential Fourier syntheses and refined isotropically. In complex **5**, hydrogens on Ru atoms were not located.

Appendix A. Supplementary data

Crystallographic Information has been deposited with the Cambridge Crystallographic Data Centre (CCDC Nos. 273654 (**1**), 273655 (**2**), 273656 (**3**), 273657 (**4**), 273658 (**5**), 273659 (**6**), and 273660 (**7**)). The data can be obtained free of charge via www.ccdc.cam.ac.uk (or from the Cambridge Crystallographic Data Centre, 12 Union Road, Cambridge CB21EZ, UK; fax: (+44) 1223 336 033; or deposit@ccdc.cam.ac.uk). Supplementary data associated with this article can be found, in the online version, at doi:10.1016/j.jorganchem.2005.10.011.

References

[1] G. Huttner, K. Knoll, Angew. Chem. Int. Ed. Engl. 26 (1987) 743.
[2] (a) G. Huttner, J. Schneider, G. Mohr, J.V. Seyerl, J. Organomet. Chem. 191 (1980) 161;
(b) F. Iwasaki, M.J. Mays, P.R. Raithby, P.L. Tailor, P.J. Wheatley, J. Organomet. Chem. 213 (1981) 185;
(c) K. Natarajan, O. Scheidstrger, G. Huttner, J. Organomet. Chem. 221 (1981) 301;
(d) K. Natarajan, L. Zsolnai, G. Huttner, J. Organomet. Chem. 220 (1981) 365;
(e) H.G. Ang, C.H. Koh, L.L. Koh, W.L. Kwik, W.K. Leong, W.Y. Leong, J. Chem. Soc., Dalton Trans. (1993) 847;
(f) H.G. Ang, S.G. Ang, S. Du, B.H. Sow, X. Wu, J. Chem. Soc., Dalton Trans. (1999) 2799.
[3] J.S. Field, R.J. Hanes, D.N. Smit, J. Chem. Soc., Dalton Trans. (1998) 1315.
[4] J. Sugiura, T. Kakizawa, H. Hashimoto, H. Tobita, H. Ogino, Organometallics 24 (2005) 1099.
[5] (a) H. Lang, L. Zsolnai, G. Huttner, J. Organomet. Chem. 282 (1985) 23;
(b) K. Knoll, G. Huttner, L. Zsolnai, J. Organomet. Chem. 312 (1986) C57;
(c) K. Knoll, G. Huttner, L. Zsolnai, O. Orama, J. Organomet. Chem. 327 (1987) 379.
[6] R.A. Bartlett, H.V.R. Dias, K.M. Flynn, M.M. Olrnstead, P.P. Power, J. Am. Chem. Soc. 109 (1987) 5699.
[7] (a) J. Schneider, L. Zsolnai, G. Huttner, Chem. Ber. 115 (1982) 989;
(b) A.J. Arce, R. Machado, Y.D. Sanctis, T. Gonzáles, R. Atencio, A.J. Deeming, Inorg. Chim. Acta 344 (2003) 123.
[8] A.J. Deeming, S. Doherty, N.I. Powell, Inorg. Chim. Acta 1998 (1992) 469.

[9] (a) F.A. Cotton, Inorg. Chem. 5 (1966) 1083;
(b) R. Roulet, Chimia 50 (1996) 629;
(c) G. Bondietti, G. Laurenczy, R. Ros, R. Roulet, Helv. Chim. Acta 77 (1994) 1869.

[10] (a) R.M.D. Silva, M.J. Mays, G.A. Solan, J. Organomet Chem. 664 (2002) 27;
(b) H.-G. Ang, L.-L. Koh, Q. Zhang, J. Chem. Soc., Dalton Trans. (1995) 2757;
(c) A.A. Cherkas, J.F. Corrigan, S. Doherty, S.A. MacLaughlin, F.V. Gastel, N.J. Taylor, A.J. Carty, Inorg. Chem. 32 (1993) 1662;

(d) J.S. Field, R.J. Haines, F. Mulla, J. Organomet. Chem. 389 (1990) 227;
(e) J.S. Field, R.J. Haines, U. Honrath, D.N. Smit, J. Organomet. Chem. 329 (1987) C25;
(f) F.V. Gastel, N.J. Taylor, A.J. Carty, J. Chem. Soc., Chem. Commun. (1987) 1049.

[11] T. Oshikawa, M. Yamashita, Chem. Ind. (Lond.) (1985) 126.

[12] G.M. Sheldrick, SHELXS-97, Programs for Solving X-ray Crystal Structures, University of Göttingen, 1997.